3.6

MM-WAVE RADAR STRUCTURE AND MICROPHYSICAL CHARACTERISTICS OF MIXED PHASE ALTOCUMULUS CLOUDS

Larry R. Belcher[1*], Lawrence D. Carey[1], John M. Davis[2], J. Adam Kankiewicz[2], and Thomas H. Vonder Haar[2]

[1] Department of Marine, Earth and Atmospheric Sciences
North Carolina State University
Raleigh, NC

[2] Cooperative Institute for Research in the Atmosphere (CIRA)
Colorado State University
Fort Collins, CO

1. INTRODUCTION

Altocumulus and altostratus clouds cover 22% of the earth (Warren et al., 1988a,b) and in turn, influence the earth's albedo and climate. Yet these mixed phase clouds have been studied far less than boundary layer or cirrus clouds. Since they rarely produce precipitation or severe weather, mid-level mixed phase clouds are the "forgotten clouds" in atmospheric science. Efforts aimed at a better understanding of cloud morphology, microphysics, and lifecycle serve to improve our ability to model and forecast these clouds, which can also impact military and civilian aviation. Satellite missions (e.g., CLOUDSAT; Stephens et al. 2002) that seek to estimate cloud properties on a global scale will benefit from knowledge of the horizontal and vertical distribution of ice and liquid water in mixed-phase clouds.

The ninth Complex Layered-Cloud Experiment (CLEX-9), conducted over western Nebraska from 8 October to 4 November 2001 provided in-situ microphysical and radar measurements of mid-level clouds from the University of Wyoming King Air research aircraft (UWKA). The 95-GHz Wyoming Cloud Radar (WCR) was deployed on the UWKA providing highly resolved radar reflectivity observations. The UWKA also measured in-cloud thermodynamic state and microphysical parameters including cloud liquid water (LWC) and ice water contents (IWC) from a suite of microphysical probes (e.g., PMS 2D-C, 2D-P, and Gerber PVM). Integration of the in-situ and radar data provides the opportunity to investigate cloud morphology and the microphysical characteristics of the mixed phase clouds sampled during CLEX-9.

2. CLOUD RADAR OBSERVATIONS

The UWKA flew on 8 mission days during the CLEX-9 campaign. Radar and in-situ data were collected from numerous mid-level clouds using several sampling techniques (e.g., straight/level flight legs, straight-line ascents, and Lagrangian spirals) during each sortie. The WCR data provide a highly resolved view of cloud structure and complements the in-situ microphysical measurements. The WCR cross-section (Fig. 1) captures the cellular structure showing enhanced regions of reflectivity associated with cloud ice, cascading into the sheared lower cloud region. The cells (and associated fallstreaks) exhibit a periodicity across the flight leg, analogous to the clusters of enhanced ice regions observed by Hobbs and Rangno (1985) in stratiform clouds. The periodicity of these enhanced ice regions, and their correlation with cloud top microphysical measurements will be investigated in Section 4 of this study.

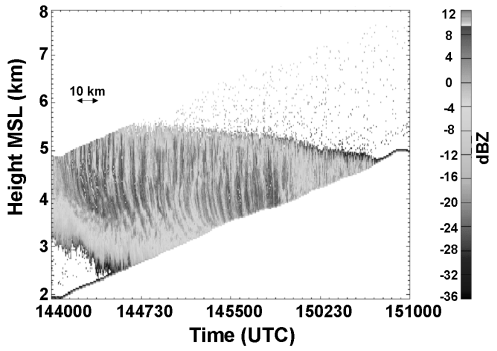

Figure 1. WCR reflectivity vertical cross-section during a straight-line ascent on 14 October 2001 from 1440 to 1510 UTC.

The WCR data also provide the opportunity to investigate the spatial and temporal variability of cloud IWC in mixed phase clouds. Estimates of IWC depend on an accurate determination of *a* and *b* terms shown in Equation (1), relating measured reflectivity to IWC.

$$IWC = aZ^b \quad (1)$$

The IWC-Z relationship was determined based on a linear regression between normalized IWC and the equivalent reflectivity (Z_e). Estimates of IWC (and Z_e) were obtained using the "all-snow" mass-dimensional relationship found by Mitchell et al. (1990), and integrating over the 2D-C particle size distribution (PSD)

**Corresponding author's address:*
Larry R. Belcher, North Carolina State University, Raleigh, NC 27695, E-mail: larry_belcher@ncsu.edu

data. We have calculated *a* and *b* values for each case day to minimize potential error due to PSD variability on a given day.

The best estimator for the 14 October (Eq. 2.) case was applied to the WCR data from the flight leg shown above (i.e., 1440-1510 UTC) to obtain a vertical profile of IWC.

$$IWC = 0.0087Z^{0.531} \quad (2)$$

The results are presented as a contoured frequency by altitude diagram (CFAD; Yuter and Houze, 1995) shown in Figure 2.

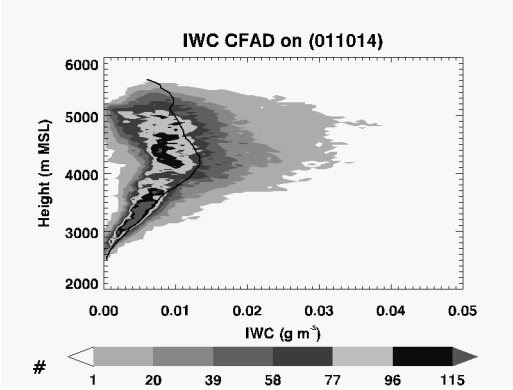

Figure 2. Contoured Frequency by Altitude Diagram (CFAD) of WCR-derived IWC from 14 October 2001 during a straight-line ascent at 1440 through 1510 UTC. The CFAD was constructed using a 30 m vertical resolution with 0.001 g m^{-3} bins. The mean IWC at each level is shown as a solid line.

The estimated IWC values for this case fall below 0.04 g m^{-3} with the largest values residing from 4 to 5 km (all heights MSL). The vast majority of IWC values are below 0.01 g m^{-3} at all levels. The average profile shows a peak value of 0.013 g m^{-3} at an altitude of 4200 m. The overall trend in the CFAD suggests that the highest concentrations of cloud ice reside in the middle to lower portion of the cloud (i.e., below 4700 m).

3. CLOUD MICROPHYSICS

Fleishauer et al. (2002) investigated the microphysical properties of mid-level clouds (e.g., altocumulus clouds) during the fifth Complex Layered-Cloud Experiment (CLEX-5). They observed and documented numerous mid-level clouds, which typically exhibited maximum values of LWC at cloud top, consistent with previous work (e.g., Heymsfield et al., 1991; Rauber and Tokay 1991, Hobbs and Rangno, 1998). Their results also indicated that maximum values of estimated IWC resided in the mid to lower cloud regions of single layered clouds, consistent with the CFAD results (Fig. 2) discussed above.

The vertical profile of LWC and IWC (Fig 3.) from the 14 October (1440-1510 UTC) flight leg further confirms consistency between the CLEX-9 observations and previous work. The peak LWC values of 0.22 g m^{-3} reside at an altitude of 4900 m and temperature of –20 °C (i.e., near cloud top). The mixed phase region of the cloud is several hundred meters thick with profiles of temperature and dew point temperature (not shown) indicating supersaturated conditions. Peak IWC values reach 0.1 g m^{-3} and occur at –12°C, which is the temperature corresponding to the maximum difference between the saturated vapor pressure over water and ice. Immediately following this ascent, the UWKA began a descending Lagrangian spiral. The vertical profiles of in-situ observations from the descending spiral (not shown) are consistent with those presented during the ascent.

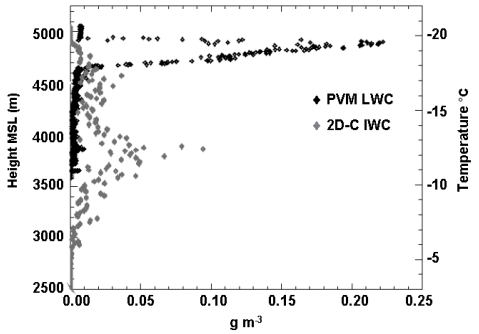

Figure 3. The vertical profile of LWC (black diamonds) and IWC (gray diamonds) during the 14 October 2001 straight-line ascent from 1440 to 1510 UTC. LWC data shown here are from the Gerber PVM and IWC data are from the PMS 2D-C spectra using Mitchell et al. 1990 M-D relationship.

The PSD of water droplets and ice particles throughout the cloud provides more details on cloud microphysical characteristics. The PSD of cloud water droplets (from the FSSP-100) and ice particles (from the 2D-C) at mid-cloud and cloud top are shown in Fig. 4. There was no liquid water (Fig. 3) at mid-cloud yet the FSSP did record a few particles at the largest size bin (30 μm) that were likely due to ice contamination. The 2D-C shows a bi-modal distribution (Fig. 4b) of ice particles with peaks at 300 and 600 μm and a long tail out to 2500 μm. This picture reverses at cloud top, with the cloud droplet PSD normally distributed, ranging from 5 to 25 μm (Fig. 4a) and much lower ice concentrations. Interestingly, the ice PSD is multi-modal at cloud top with maxima near 175, 350, and 700 μm. Particle imagery from the 2D-C near cloud top in the mixed phase region where LWC peaked show the presence of ice in the form of sector plates and other plate like crystals (Fig. 5a), as expected for the observed temperatures. PMS 2D-C particle imagery at mid-cloud near the IWC and reflectivity maxima reveal the presence of large plate like crystals, some in the form of aggregates (Fig. 5b).

These observations clearly show the existence of a cloud top liquid layer proposed by Rauber and Tokay (1991). The liquid layer serves as the source region for the generation of ice crystals. Nucleation likely occurs via contact nucleation (Young, 1974) as postulated by Hobbs and Rangno (1985) when cloudy and ambient air mixes near cloud top, resulting in the partial evaporation

and freezing of a small fraction of larger (> 20 μm, Fig. 4a) droplets. The nucleated ice likely grew rapidly via deposition and aggregation in a moisture rich environment, reaching sizes up to 2000 μm, and gravitationally settled to lower levels of the cloud.

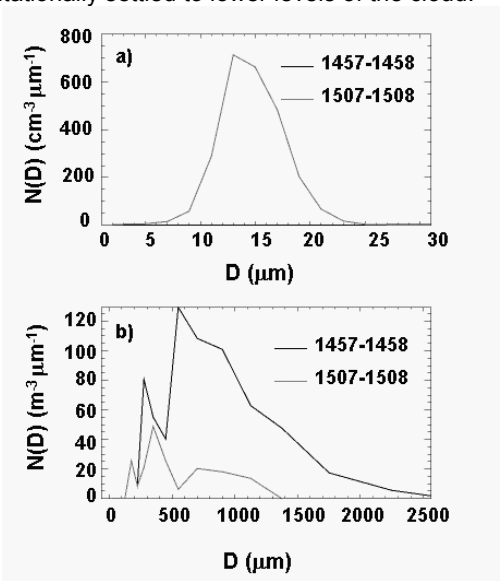

Figure 4. Cloud liquid water droplet spectra (a; FSSP-100) and cloud ice spectra (b; PMS 2D-C) during the 14 October 2001 straight-line ascent from 1440 to 1510 UTC. The total recorded PSD during a 1 minute period at mid-cloud (1457-1458, black line) and near cloud top (1507-1508, gray line) are shown.

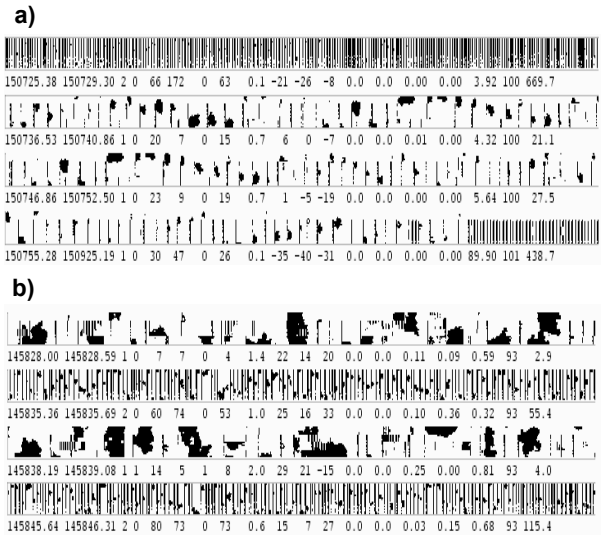

Figure 5. Cloud particle imagery from the PMS 2D-C during the 14 October 2001 straight-line ascent from 1440 to 1510 UTC. a) 1507:25-1507:55 as UWKA entered the region of highest LWC near cloud top and b) 1458:28-1458:45 as UWKA entered the region of highest radar reflectivity and IWC at mid-cloud.

4. CLOUD HOMOGENEITY

The WCR cross-section presented above (Fig. 1) shows enhanced regions of reflectivity dispersed along the flight line, a feature common to many of the CLEX-9 radar observations. Similarly, the microphysics probes also exhibit spikes during in-cloud flight legs. Hobbs and Rangno (1985) found regions of high ice concentrations in clusters with horizontal dimensions up to 100 m, leading to the conclusion that cloud ice forms in these clusters in tufts near cloud top. Investigation of the periodicity of these clusters at various levels within the cloud provides further insight into cloud morphology, microphysical mechanisms and horizontal homogeneity.

During a second (afternoon) mission on 14 October 2001, the UWKA conducted a straight and level flight-leg along cloud top at 5223 m (1730 to 1740 UTC) during a Terra satellite overpass (Fig. 6). Prior to the satellite overpass, the UWKA flew a straight-line ascent providing a WCR cross-section through this cloud once again capturing the cellular structure (Fig. 7). Time series plots of FSSP concentration (Fig. 8a) and Gerber PVM LWC (Fig 8b) data from 1730 to 1740 UTC show the response of each instrument as the aircraft passes through moisture rich clusters along the flight leg. Similarly, the time series plot of reflectivity (Fig. 8c) from 1722 to 1730 UTC exhibit spikes of enhanced reflectivity along the flight track (reflectivity data were collected at one second intervals in a 50 m altitude window centered at 4975 m).

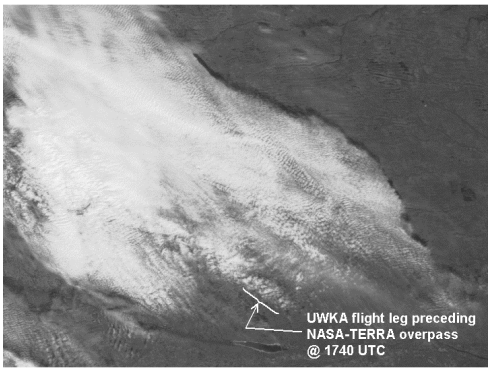

Figure 6. Moderate Resolution Imaging Spectroradiometer (MODIS) image of cloud sampled by UWKA during Terra satellite overpass on 14 October 2001 at 1742 UTC (*Image courtesy of MODIS Rapid-Response Team at NASA-GSFC)*.

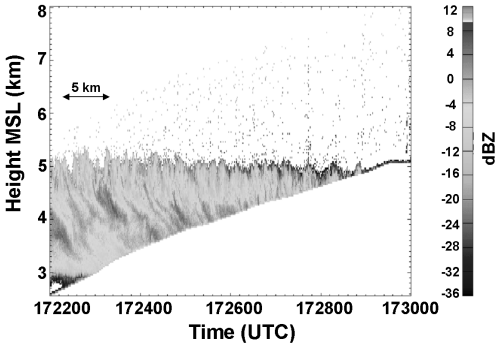

Figure 7. WCR reflectivity vertical cross-section during a straight-line ascent on 14 October 2001 from 1722 to 1730 UTC.

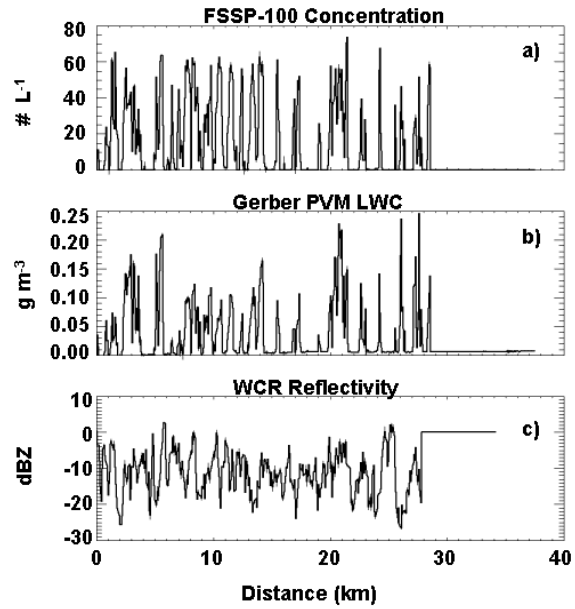

Figure 8. Time series plots of (a) FSSP concentration, and (b) Gerber PVM LWC from 1730-1740 UTC near cloud top at 5223 m MSL, and (c) WCR reflectivity from 1722-1730 UTC below cloud top at 4975 m MSL on 14 October 2001. Note that each time series is plotted with respect to distance traveled over the flight leg in the noted time frame, based on the average aircraft speed.

Each of the instruments is responding to enhanced regions of liquid (and ice in the case of the WCR) within the cloud as indicated by the time series plots. However the frequency of each instrument's response is not readily apparent by eye and requires further investigation. We have conducted spectral analysis using the SSA (Singular Spectrum Analysis) toolkit (Ghil et al., 2002) to retrieve the periodic behavior of each time series shown above. The analyses indicate that the FSSP, PVM, and WCR data oscillate with periods of 1400, 1500, and 1100 m respectively. These periods were found to be statistically significant in each case. The reasonable agreement found here confirms the connection between the liquid layer at cloud top and the enhanced ice region lower in the cloud, occurring in clusters throughout the cloud.

5. CONCLUSIONS

Integration of the in-situ and radar data has provided the opportunity to investigate the structure and microphysical characteristics of mixed phase clouds sampled during CLEX-9. The results found here agree well with previous observational studies (e.g., Hobbs and Rangno, 1985, 1998; Heymsfield et al., 1991; Fleishauer et al., 2002), which showed typical cloud structure was comprised of a liquid layer at cloud top serving as a source region for ice crystal production. The cellular structure indicates that the liquid drops and ice are distributed in clusters within the clouds at somewhat regular intervals. Observations of LWC and IWC from the 14 October 2001 case study reached values near 0.23 and 0.1 g m^{-3} at cloud top and mid-cloud levels respectively. A broad PSD of liquid droplets was observed at cloud top while the magnitude and breadth of ice PSD increased with decreasing altitude within the cloud to about mid-cloud level.

The WCR data served to complement the in-situ observations and captures the cellular structure of the clouds investigated here. We have also utilized the radar data to provide reasonable estimates of IWC over the entire cloud. The radar and in-situ data also provided a means to estimate the periodic behavior of the generating cells. However, the results found here were from a limited sample from the extensive CLEX-9 data set. Future work will continue to investigate additional cases in order to augment the observational database of mid-level mixed phase clouds.

6. ACKNOWLEDGEMENTS

We would like to thank all personnel on the CLEX-9 team for their efforts to make this study possible. The Department of Defense sponsored Center for Geosciences/Atmospheric Research at Colorado State University supported this work through research agreements G-7460-1 and G-7404-1.

7. REFERENCES

Fleishauer, R. P., V. E. Larson, T. H. Vonder Haar, 2002: Observed Microphysical Structure of Midlevel, Mixed-Phase Clouds. *J. Atmos. Sci,,* **59**, 1779-1804.

Ghil, M., M. R. Allen, M. D. Dettinger, K. Ide, D. Kondrashov, M. E. Mann, A. W. Robertson, A. Saunders, Y. Tian, F. Varadi, and P. Yiou, 2002: Advanced spectral methods for climatic time series. *Rev. Geophys.*, **40**(1), 1003, 10.1029/2000RG000092.

Heymsfield, A. J., L. M. Miloshevich, A. Slingo, K. Sassen, and D. O'C. Starr, 1991: An observational and theoretical study of highly supercooled altocumulus. *J. Atmos. Sci.*, **48**, 923-945.

Hobbs, P. V., and A. L. Rangno, 1985: Ice particle concentrations in clouds. J. Atmos. Sci., 42, 2523-2549.

—— and ——, 1998: Microstructures of low and middle-level clouds over the Beaufort Sea. *Quart. J. Roy. Meteor. Soc.*, **124**, 2035-2071.

Mitchell, D. L., R. Zhang, and R. Pitter, 1990: Mass-dimensional relationships for ice particles and the influence of riming on snowfall rates. *J. Appl. Meteor.,* **29,** 153–163.

Rauber, R. M., and A. Tokay, 1991: An explanation for the existence of supercooled water at the tops of cold clouds. *J. Atmos. Sci.,* **48,** 1005–1023.

Stephens, G. L., D. G. Vane, R. J. Boain, G. G. Mace, K. Sassen, Z. Wang, A. J. Illingworth, E. J, O'Connor, W. B. Rossow, S. L. Durden, S. D. Miller, R. T. Austin, A. Benedetti, C. Mitrescu, 2002: The CLOUDSAT mission and the A-TRAIN, *Bull. Amer. Meteor. Soc.,* **83,** 1771-1790.

Warren, S. G., C. J. Hahn, J. London, R. M. Chervin, and R. Jenne, 1988a: Global distribution of total cloud cover and cloud type amount over land. NCAR Tech. Note TN-317 STR, 212 pp.

——, ——, ——, ——, and ——, 1988b: Global distribution of total cloud cover and cloud type amount over the ocean. NCAR Tech. Note TN-317 STR, 212 pp.

Young, K. C., 1974: The role of contact nucleation in ice phase initiation in clouds. *J. Atmos. Sci.*, **31**, 768-776.

Yuter, S. E. and R. A. Houze Jr., 1995: Three-dimensional kinematic and microphysical evolution of Florida cumulonimbus. Part II: Frequency distributions of vertical velocity, reflectivity, and differential reflectivity. *Mon. Wea. Rev.,* **123**, 1941-1963.